Hindawi
Science and Technology of Nuclear Installations
Volume 2019, Article ID 4936379, 10 pages
https://doi.org/10.1155/2019/4936379

Research Article

Effect of Fe_2O_3 on the Immobilization of High-Level Waste with Magnesium Potassium Phosphate Ceramic

Hailin Yang,[1,2] **Mingjiao Fu**,[3] **Bobo Wu**,[4] **Ying Zhang**,[2] **Ruhua Ma**,[2] **and Jueshi Qian**[1]

[1]*College of Materials Science and Engineering, Chongqing University, Chongqing 400045, China*
[2]*College of Environment and Resources, Chongqing Technology and Business University, Chongqing 400067, China*
[3]*Guizhou Aerospace XinLi Casting and Forging Co., LTD, Zunyi, Guizhou Province 563000, China*
[4]*Zunyi Transportation and Tourism Investment, Zunyi, Guizhou Province 563000, China*

Correspondence should be addressed to Hailin Yang; hailinyang@gmail.com

Received 28 September 2018; Accepted 30 December 2018; Published 3 February 2019

Guest Editor: Rema Abdulaziz

For the proposed novel procedure of immobilizing HLW with magnesium potassium phosphate cement (MKPC), Fe_2O_3 was added as a modifying agent to verify its effect on the solidification form and the immobilization of the radioactive nuclide. The results show that Fe_2O_3 is inert during the hydration reaction. It slows down the hydration reaction and lowers the heat release rate of the MKPC system, leading to a 3°C-5°C drop in the mixture temperature during hydration. Early comprehensive strength of Fe_2O_3 containing samples decreased slightly while the long-term strength remained unchanged. For the sintering process, Fe_2O_3 played a positive role, lowering the melting point and aiding the formation of ceramic structure. $CsFe(PO_4)_2$, or $CsFePO_4$, was generated by sintering at 900°C. These products together with the ceramic structure and absorption benefit the immobilization of Cs^+. The optimal sintering temperature for heat treatment is 900°C; it makes the solidification form a fired ceramic-like structure.

1. Introduction

The utilization of nuclear energy resulted in the accumulation of large amounts of liquid high-level radioactive waste (HLW) which contains environmentally hazardous elements like plutonium and other actinides in addition to fission and corrosion products [1]. Safe disposal of HLW is of key concern in the application of nuclear energy. The dominant technology for the solidification of HLW is vitrification. Generally, the technology of immobilizing HLW through vitrification does not ensure the complete immobilization of radionuclides due to the low hydrothermal stability of the glass produced [2]. In recent research, the incorporation of radionuclides into crystalline phases (pyrochlore, zircon, zirconolite, etc.) that are analogs to natural minerals and that have high radiation and chemical stability is considered as an alternative way for vitrification. Various methods were proposed for the preparation of mineral-like matrices, e.g., cold pressing and sintering or hot pressing or induction melting in a cold crucible [3]. As alternative materials for vitrification, various matrices were proposed for immobilization of HLW including hydrothermal synthetic rock [4–6], ceramics [2], and Portland cement [7].

Magnesium phosphate cements (MPCs) are cementitious materials that are formed through a solution acid-based reaction between dead burnt magnesia and phosphate. Retarder and mineral admixtures may be added during hydration reaction to achieve proper workability or specific properties [8–10]. Formed at ambient temperatures and exhibiting properties like ceramics, MPCs are also termed chemically bonded phosphate ceramics [11]. MPCs have several advantages over conventional Portland cement such as rapid setting time, high early strength, good bonding with Portland cement, little drying shrinkage, and better resistance to abrasion, etc. [12]. These superior properties lead MPCs to be widely used in various engineering structures, especially in emergency-repairing as well as in the solidification of hazardous materials [13].

Earlier MPCs featured a "two-part" system, consisting of dead burnt magnesia and a soluble orthophosphate, i.e., $NH_4H_2PO_4$ (ADP) or KH_2PO_4 (KDP) [14]. However, the hydration reaction is too fast to allow enough time for

operation. Subsequently, a "three-part" MPC system based on magnesium and phosphate was prepared with the addition of retarders [15]. The use of sodium triphosphate (STP), boric acid (H_3BO_3), or borax ($Na_2B_4O_7{\cdot}10H_2O$) as retarders has been reported in recent literature [16, 17]. Particularly, borax has been widely used in academic study and commercial application due to its easy storage and effectiveness [8].

Since the reaction between MgO and ADP releases ammonia, in consideration of the secondary pollution control, we prefer to adopt the magnesium potassium phosphate system as the raw material. The hydration reaction is governed by [18]

$$MgO + KH_2PO_4 + 5H_2O \longrightarrow MgKPO_4 \cdot 6H_2O \quad (1)$$

Nuclear reactors periodically unload spent fuel containing unburnt nuclear fuel, abundant fission fragments, and their decay products [19]. To achieve intensive utilization of limited uranium resources, spent fuel should be recycled by postprocessing such as PUREX [20]. Postprocessing discharges aqueous HLW that carries most of the radioactive activity and toxicity from the spent fuel, making aqueous HLW the most important radioactive waste that needs to be handled.

As shown in the reaction equations, aqueous HLW could be directly immobilized by the introduction of binding agents. The cement-like solidification process is characterized by its low energy inputs, the simplicity of realization, as well as the minimization of secondary radioactive waste, and the low mobility of the nuclide ion. Compared to conventional cementation, MKPC has perceptible advantages: possibility of solidifying liquid wastes within a wide range of pH, high loading capacity toward HLW, etc. Interest in the use of binding phosphate materials for radioactive waste immobilization has risen during last few years. Singh et al. investigated immobilizing ^{99}Tc with MKPC Ceramicrete. The solidified form was achieved and had a comprehensive strength no less than 30 MPa. The solidification mechanism of ^{99}Tc was proven to be the combination of mechanical enclosing and chemosetting [21]. Vinokurov et al. studied to solidify simulated HLW with MPC at ambient temperatures. Results show that the density of solidified form is 1.7 g/cm^3 while its comprehensive strength exceeds 20 MPa. The leaching resistance conforms to relevant standards [1]. Wagh et al. attempted to solidify radioactive waste containing Pu with MPC. Pu^{3+} was translated into Pu^{4+} (Insoluble oxide) first to reduce the solubility and then achieve better immobilization. Testing shows that Pu^{4+} was well immobilized through both the chemical stabilization and the physical encapsulation [22, 23].

Scientists of ANL (USA) offered the use of phosphate materials (Ceramicrete) for immobilization of low-level and technetium-containing simulant waste solutions as well as for incorporation of Pu-containing ash. At the Khlopin Radium Institute (Russia) and INEEL (USA), the possibility of incorporating a simulant of low-level ash remainder of combustible radioactive waste into iron phosphate matrices was also studied [1].

In our previous study, a novel procedure of HLW immobilization was developed in which the liquid HLW was added as a substitute for the mixing water of the MKPC system. This procedure makes the processing very simple and direct. The solidified form has advantages over glass solidification or synroc solidification in terms of chemical stability and heat resistance, etc. Further study showed that the MKPC solidification form has good thermal resistance; it keeps intact even after sintering at 1400°C for hours, and the sintering makes MKPC form into real fire ceramics. In consideration of the heat releasing of the HLW, the MKPC form needs to withstand quite high temperatures after the HLW disposal. So, we believe that the presintering is beneficial for the durability and stability of the solidified forms as well as for the immobilization of the nuclide.

Iron phosphate has been proven to be appropriate for hazardous material immobilization. Sales, B. C. et al. reported that the lead-iron phosphates glass performs well as stable storage of high-level nuclear waste [24]. Greaves, G. N. et al. added iron oxide to prepare lead-iron-phosphate glasses and to achieve more stable structure [25]. Mechanically, iron ions can enter the network structure of phosphate, Fe^{3+}, and replace P^{5+} because of its stronger electro-positivity, thus forming a Fe - O - P bond which has better water resistance. Furthermore, the smaller radius of the iron ion (Fe^{3+}, Fe^{2+}) can hinder the larger water module from passing through the solidification form, therefore, significantly improving the chemical stability of immobilization matrix [26, 27].

Iron oxide is one of the most abundant metal oxides on earth. Its abundant and inexpensive characteristics make it a promising candidate to partially replace the magnesium for forming phosphate cements. It is meaningful to investigate the effect of fe_2o_3 on the immobilization of aqueous high-level waste with magnesium potassium phosphate ceramic. An experimental study was carried out in this paper to verify the function of the iron oxide in both the hydration reaction and the sintering process of the MKPC matrix.

2. Materials and Experiments

2.1. Materials. The magnesium potassium phosphate cement paste was prepared through a mixture of dead burnt magnesium oxide (MgO), acidic phosphate (KDP), and borax in specific proportions. The chemical characteristics of the raw materials are listed in Table 1.

The aqueous HLW considered in this study is the effluent of spent fuel postprocessing. During the postprocessing procedure, the spent fuel from the nuclear power reactor is mechanically cut and then dissolved in nitric acid. The solution is then filtered and clarified, and residual U and Pu are extracted for recycling by extraction agents, e.g., TBP. The aqueous HLW is discharged by spent fuel recycling and posttreatment processes. Generally, it is a mixture of concentrated nitric acid and various kinds of nitrate solution that contain the majority of the radiation and toxicity of the spent fuel. Due to the safety considerations and experimental conditions, a simulated aqueous HLW was used to represent the nuclear power reactor aqueous HLW. Cations were introduced into nitric acid by corresponding nitrate. Nuclides

Table 1: Characteristics of raw materials.

Component	Characteristics	Supplier
Dead burnt magnesium oxide powder (MgO)	Industrial grade, >95% MgO	Liaoning Xinrong Mining Group Co. Ltd., China
KDP (KH_2PO_4)	Industrial grade, >98% KDP	Qingzhou Guanghui Chemical Plant Co. Ltd, China
Borax ($Na_2B_4O_7{\cdot}10H_2O$)	Industrial grade, >95% borax	Tibet Pengdu Boron Industry Co. Ltd., China

Table 2: Composition of typical power nuclear reactor aqueous HLW (g/L) [28].

Al^{3+}	Ba^{2+}	Cr^{3+}	Fe^{3+}	K^{+}	Na^{+}	Cs^{+}	Ni^{2+}	Sr^{2+}	Mo^{6+}	Ce^{3+}	Nd^{3+}
15.9	0.074	2	17.4	0.45	51.2	2	8.2	0.61	0.82	0.78	2.05

[a] C_{HNO3}=2.6 mol/L.

Table 3: Basic formula of MKPC.

Component	MgO	KDP	Borax	Water
Ratio	100	25	12	16

were represented by their nonradioactive isotopes. We believe this is appropriate in chemical view. The simulated aqueous HLW was prepared according to the composition listed in Table 2.

$K_3PO_4{\cdot}7H_2O$ was introduced into aqueous HLW to adjust the pH value in advance. Fe_2O_3 powder was mixed with MgO homogeneously as an additive. All above-mentioned chemicals are analytically graded products.

2.2. Experiments. Solidified blocks were prepared through the following steps. (1) Add $K_3PO_4{\cdot}7H_2O$ into aqueous HLW to adjust pH to the specific value. (2) Add KDP and Borax into the liquid HLW at specific proportion and stir to make the liquid (solution and sediment) a homogeneous mixture. (3) Add mixture of MgO and Fe_2O_3 into the liquid and stir the hydration reaction. Pour the paste into cubic mold when the flowability is appropriate. (4) Vibrate by hand, use glass rod to densify paste, and avoid the opening. (5) Cure at ambient room temperature for hours. (6) Remove mold and retrieve blocks for further processing and study. (7) After ambiently curing for 7 days, the solidification forms were sintered for 2 hours at specific temperature in a muffle furnace. Heating rate of the muffle furnace was set to 5°C/min.

The basic formula of MKPC was listed in Table 3.

Hydration heat release was tested by an eight-channel micro calorimeter (Thermonetrics TAMair). The compressive strength of the hardened blocks was measured according to the standard of *method of testing cement-determination of strength* (idt ISO 679:1989). The strength of the samples at the ages of 1 h, 3 h, 1 day, 3 days, and 7 days was tested. To assure the reproducibility of experimental results, at least three replicates of specimens from each set were prepared and tested under the same conditions. The adiabatic temperature curve of the hydration reaction was recorded by an automatic temperature recorder that was dipped into the mixture while the mixture was placed into a vacuum cup. The leaching behavior of the most important nuclide, i.e., cesium, was tested according to the static immersion method of MCC-1 [29] using deionized water as the leachant and leaching at 40°C. The concentration of the Cs^{+} in the leachant was analyzed by flame atomic absorption spectrophotometer (TAS-990). The reaction product of MPC and liquid HLW were analyzed by X-ray diffraction (XRD, Panalytical xpert Powder) with a 2θ scanning rate of 0.5°/min. The microstructure and morphology of the blocks were observed by scanning electron microscopy (SEM, Hitachi 1050).

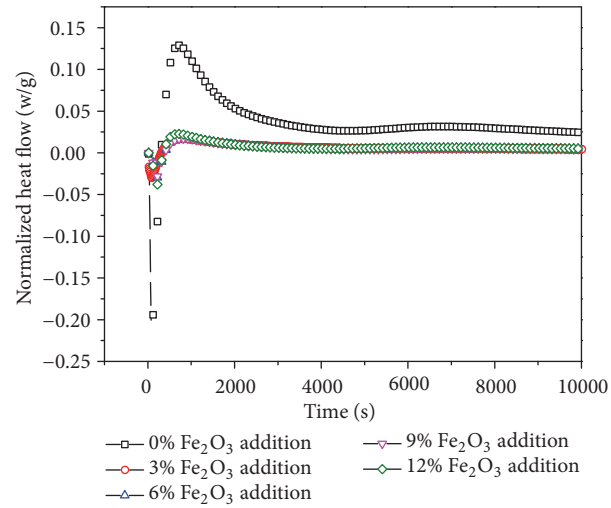

Figure 1: Exothermic curve of the mixture during hydration.

3. Results and Discussion

3.1. Effect on MKPC Systems. Fe_2O_3 was added at a dosage series of 0%, 3%, 6%, 9%, and 12% (wt% of MgO to replace MgO) to investigate the effect on MKPC hydration.

The exothermic curve of the mixture during hydration can be seen in Figure 1. The hydration heat release curve of the original MKPC has an endothermic valley and two exothermic peaks. The endothermic valley is because of the heat absorption of monopotassium phosphate's dissolution. MgO's dissolution in an acid solution as well as the hydration reaction release heat to make up the two exothermic peaks.

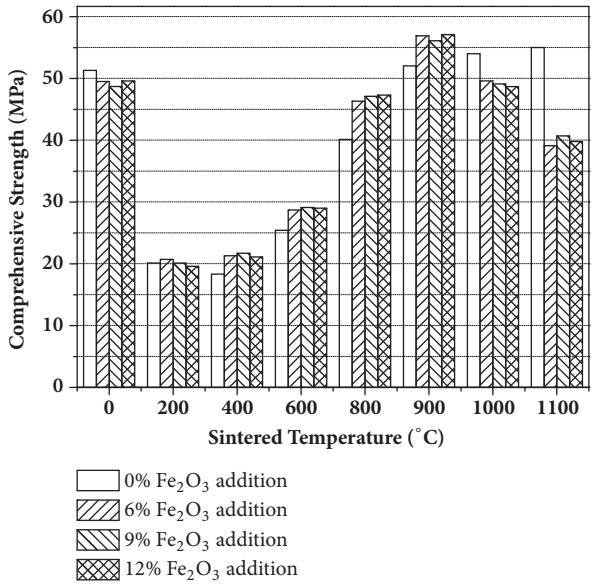

Figure 2: Comprehensive strength.

Endothermic valley keeps the same after the addition of Fe_2O_3, for the dissolution of monopotassium phosphate keeps unchanged. The addition of Fe_2O_3 reduced the heat release rate of the hydration reaction thus nearly flattening the second exothermic peak. Although Fe_2O_3 also meets the same requirements as MgO of 2n (pH) ≥pKsp to prompt the hydration reaction [30], its dissolution rate is much lower than MgO in an acid solution at room temperature. Thus, the addition of Fe_2O_3 substituted part of MgO and played the role of inert matter, resulting in a slower reaction rate and less hydration heat release rate because of the reduction of active substance, i.e., the MgO. Fe_2O_3 prolonged the setting time and lowered the exothermic curve dramatically while the overall heat releasing just changed slightly because of the reduction of MgO.

Fe_2O_3 was added at a dosage series of 0%, 6%, 9%, and 12% (wt% of MgO to replace MgO) to investigate the effect on mechanical property. Samples of the original MKPC and the sintered MKPC were tested for comprehensive strength (Figure 2). The basic result is that the addition of Fe_2O_3 does not reform the mechanical property of original MKPC remarkably. The comprehensive strength of the original samples even dropped with the addition of Fe_2O_3. Sintering at no more than 800°C weakened the comprehensive strength of samples. This is due to the sintering destroying the original structure, but not leading to a solid melting reaction due to the temperature not being high enough. Sintering at 900°C hardened the samples because of the melting reaction forming ceramic microstructure. 1000°C and 1100°C sintering hardened the original sample while weakening the Fe_2O_3 containing samples. Both the original and Fe_2O_3 containing samples were macroscopically destroyed by 1200°C sintering. The addition of Fe_2O_3 hardened the sintered samples at a temperature range of no more than 900°C while its effect was negative for the original samples. The proposed mechanism is that Fe_2O_3 is inert matter for the hydration reaction, but it lowers the melting temperature of system remarkably. When considering sintering in the whole immobilization process, Fe_2O_3 does benefit the mechanical property of the MKPC solidification form.

3.2. Effect on HLW Immobilization. Aqueous HLW was used to substitute mixing water completely in the proposed immobilization procedure. Since liquid HLW is a very concentrated acid liquor (pH<1), it may degrade the cement system and lead to failure of the immobilization. So the liquid HLW was treated in advance to adjust its pH value. $K_3PO_4{\cdot}7H_2O$ was used as buffer agent since its solution is alkalic and the introduction of $K_3PO_4{\cdot}7H_2O$ does not bring in extra elements. The neutralization reaction produces the sediment nuclide phosphate, which is more stable than hydroxide. Thus, the pretreatment benefits immobilization and eliminates the negative effect of nitric acid.

HLW was pretreated to specific pH (3, 5, 7) and then incorporated into the MKPC system mix water to form solidification blocks. Original samples and samples containing 9% Fe_2O_3 were tested to find the effect of Fe_2O_3 on the immobilization form.

As can be seen in Figure 3, comprehensive strength test indicated that the addition of Fe_2O_3 reduced early strength (age < 1 d) dramatically while the long-term strength was almost the same as original solidification forms at all pH levels. This is due to the fact that Fe_2O_3 substituted MgO as an inert matter and then reduced the generation of the K-struct struvite, i.e., $MgKPO_4{\cdot}6H_2O$. At the same time, it slowed down the hydration reaction. Both effects harmed the early strength. Long-term strength stood unchanged because the dosage of Fe_2O_3 was relatively low overall. Samples were sintered at 800°C, 900°C, and 1000°C to see the effect of Fe_2O_3 on sintering. The findings verified that the introduction of Fe_2O_3 lowered the melting temperature of system and reinforced the structure when sintered below 1000°C. This benefitted the sintering process through easier melting reaction and the forming of ceramic structure.

The adiabatic temperature curve of the hydration reaction was plotted. As seen in Figure 4, the curve of the Fe_2O_3 contained samples is lower and smoother than the Fe_2O_3 free samples. This indicates that at all pH levels (3, 5, 7), the introduction of Fe_2O_3 slowed down the heat release rate and lowered the equilibrium temperature and delayed the emergence of thermal balance. A reasonable explanation is that the partial substitution of MgO by Fe_2O_3 resulted in the reduction of reactant, therefore slowing down the hydration reaction. This explanation is also proven by chemical phase analysis.

The unsintered solidification form and the solidification form sintering at 900°C were prepared and analyzed by XRD. For the XRD spectrum, see Figure 5. HLW was pretreated to different pH levels (3,5,7) before mixing with the MKPC matrix. The XRD spectrum of the unsintered samples demonstrated that the iron phase shows as Fe_2O_3 and FeO·OH. This demonstrates that Fe_2O_3 is really an inert matter for hydration reaction. As to FeO·OH, it is the product of Fe_2O_3 in an alkaline environment, since MgO is superfluous according to the reaction formula and the basic

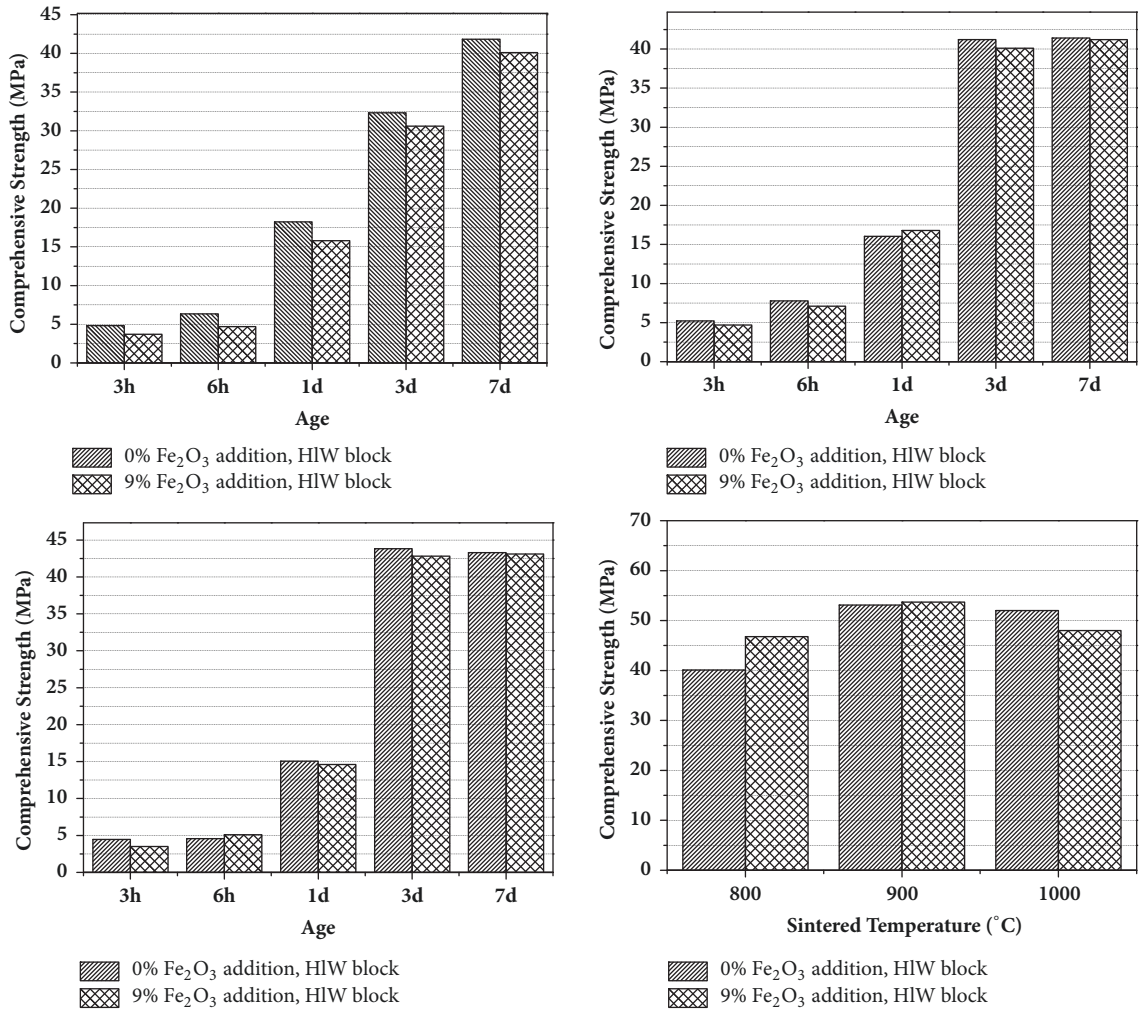

Figure 3: Comprehensive strength of solidification forms. ①HLW pH=3, ②HLW pH=5, ③HLW pH=7, ④HLW pH=5, sintered samples.

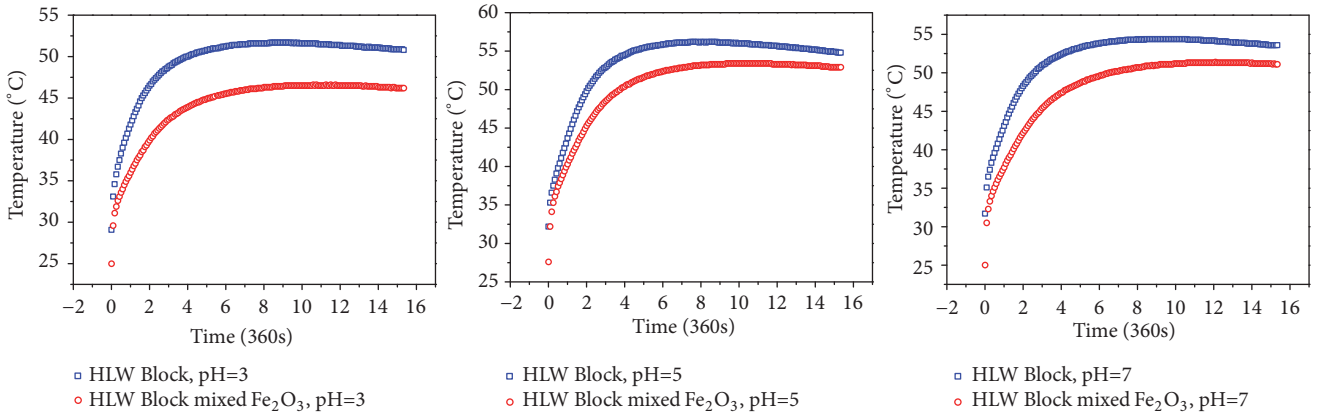

Figure 4: Adiabatic temperature curve (Fe_2O_3 dosage=9%).

matrix formula. Fe_2O_3 keeps stable at quite wide pH range. After sintering at 900°C, the characteristic diffraction peak of Fe_2O_3 and FeO·OH at the position of 2θ=21°, 2θ=34°, and 2θ=36° almost disappeared, indicating that Fe_2O_3 reacted with other constituents in the process of sintering. The HLW pH=3 diffraction peak of Fe_2O_3 is very similar to the Fe_2O_3-free samples, indicating that the addition of Fe_2O_3 barely altered the chemical phase of the solidification form. When dpH=5, the diffraction peak of $CePO_4$ moved right. A little isometric system of $CePO_4$ phase showed beside this trigonal

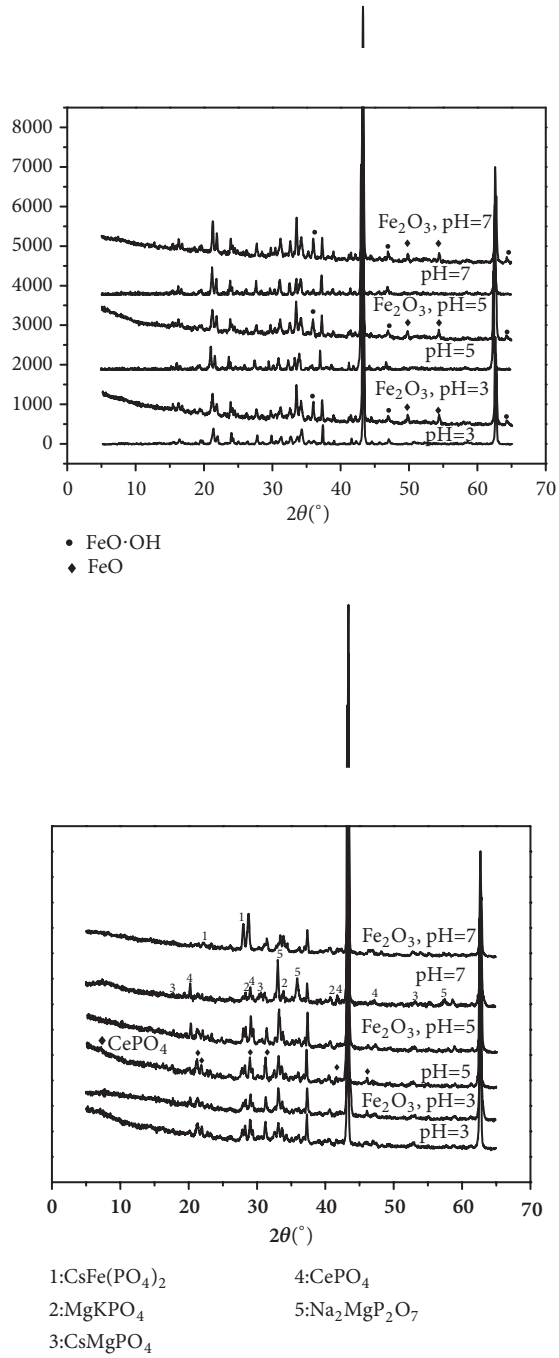

Figure 5: XRD spectrum of solidification forms (①unsintered, ②sintered at 900°C).

system. The crystallinity of the form improved. Conclusions can be drawn that the addition of Fe_2O_3 lowered the melting temperature thus producing more liquid phase at same sintering temperature benefitting the formation of ceramic structure. When pH=7, the chemical phase constitution changed dramatically. The diffraction peak at 2θ=30° rose remarkably while a new diffraction peak appeared at 2θ=20°. The new peak is verified to be $CsFe(PO_4)_2$ according to Jade software analysis.

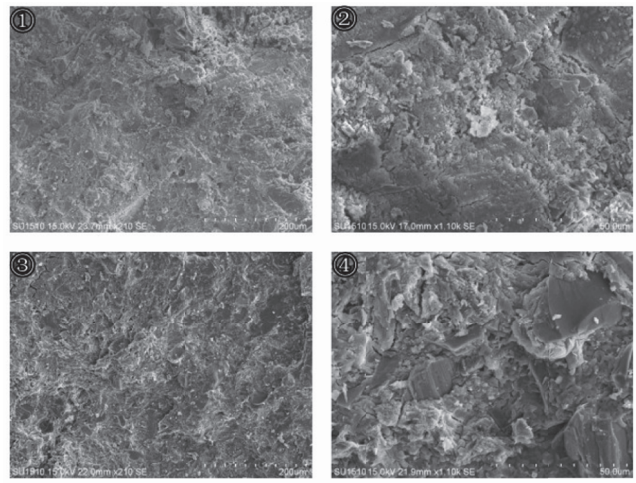

Figure 6: SEM photo of unsintered samples (HLW pH=3, ①②Fe_2O_3 free, ③④9% Fe_2O_3 addition).

In order to investigate the effect on the microstructure of the solidification form, HLW was pretreated to specific pH levels and incorporated in the MKPC matrix. The original form and Fe_2O_3 containing samples were prepared. All sample series were sintered at 900°C and compared with unsintered samples. SEM photos were taken and compared.

When HLW pH=3, the microstructure is mainly a small particle, and the crystal is underdeveloped because of the rapid hydration reaction (①② in Figure 6). Plate column and layered structure can be seen in microstructure of the Fe_2O_3 containing samples (③④ in Figure 6). As Fe_2O_3 is an inert matter, its addition reduced the content of reactant, i.e., MgO, thus slowing down the hydration reaction, making the crystal better developed and forming the plate column and layered structure.

When HLW pH=5, the crystal developed into a bigger formation. The reason is that free H^+ gets less, slowing down the reaction. The prolonged setting time makes better developed crystal (①② in Figure 7). For the Fe_2O_3 containing samples, the crystal size is smaller and mainly layered in structure, and the appearance of Fe_2O_3 reduced the production of the K-struct struvite for it is an inert matter (③④ in Figure 7).

When HLW pH=7, the crystal agglomeration region did not show on the vision field. The solidification form developed into a bigger compact plate structure. The bigger compact plate structure is a result of enough setting time for the production of K-struct struvite. The pH=7 environmentally lessens the free H^+ and benefits the crystal growth (①② in Figure 8). For Fe_2O_3 containing samples, the microstructure is compact and shown as lamellar structure (③④ in Figure 8).

As to all samples that sintered at 900°C, the microstructures present for the fire ceramic-like structure are all very compacted without visible pores (Figures 9, 10, and 11). When the HLW pH=3, Fe_2O_3 containing samples are more compacted than the Fe_2O_3 free ones, and the appearance of the iron phase lowered the melting temperature and generated more liquid phase to from ceramic structure.

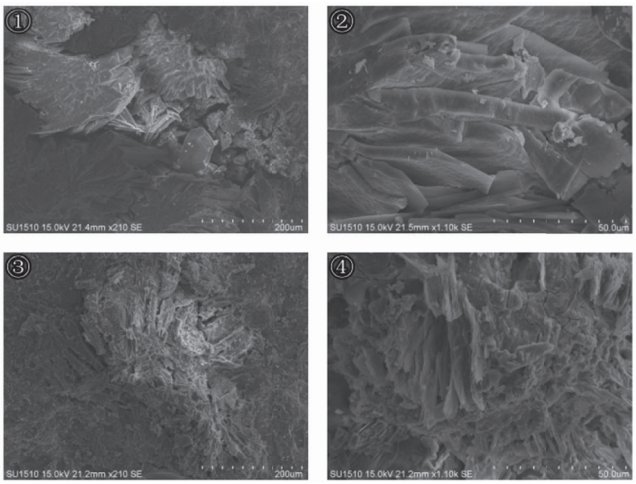

Figure 7: SEM photo of unsintered samples (HLW pH=5, ①②Fe_2O_3 free, ③④9% Fe_2O_3 addition).

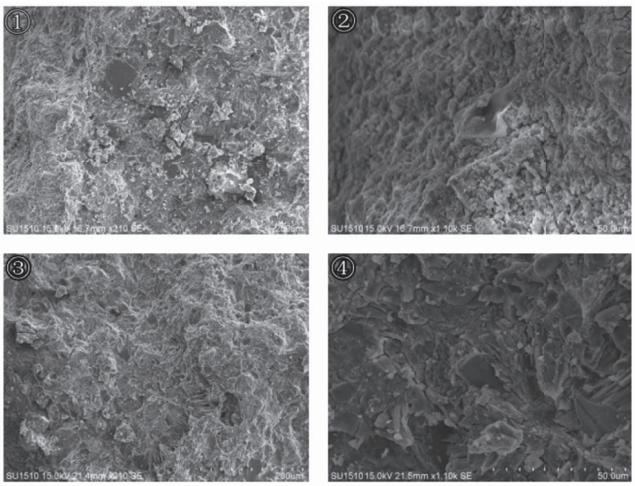

Figure 8: SEM photo of unsintered samples (HLW pH=7, ①②Fe_2O_3 free, ③④9% Fe_2O_3 addition).

When HLW pH=5, the microstructure of Fe_2O_3 containing samples interspersed with the column crystal. This deserves further investigation. When HLW pH=7, crystal grows well in Fe_2O_3-free samples, but the melting and resolidification works poorly during sintering; the microstructure is more granular. On the contrary, Fe_2O_3 containing samples show more compacted ceramic structure because of the better melting and reintegration. This is helpful for immobilization of radioactive nuclides.

According to mechanism research, immobilization of Cs^+ with MKPC system mainly depends on the following reactions. (a)Cs^+ replaces the metal ion with minor radius thus entering the crystal lattice. (b)Cs^+ is absorbed by metal phosphate. Cs^+ leaching behavior of samples containing free Fe_2O_3 and Fe_2O_3 as well as sintered and unsintered samples was tested according to the MCC-1 method. HLW was pretreated to a specific pH (3,5,7) first before being incorporated in. For the leaching rate of Cs^+, see Figure 12.

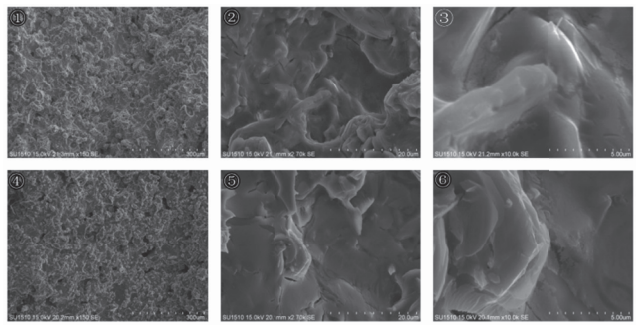

Figure 9: SEM photo of 900°C sintered samples (HLW pH=3, ①②③Fe_2O_3 free, ④⑤⑥9% Fe_2O_3 addition).

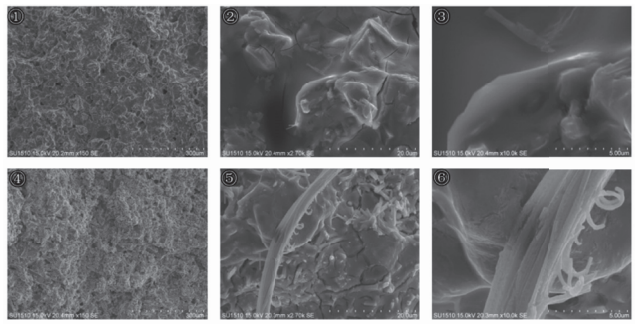

Figure 10: SEM photo of 900°C sintered samples (HLW pH=5, ①②③Fe_2O_3 free, ④⑤⑥9% Fe_2O_3 addition).

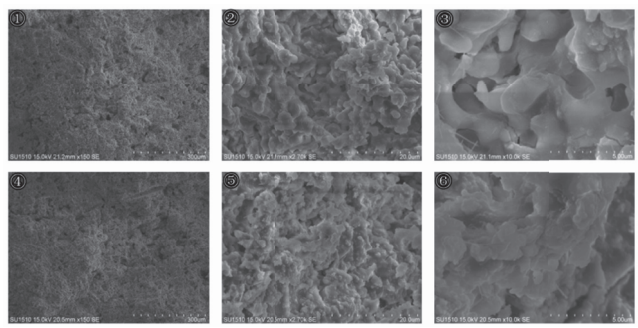

Figure 11: SEM photo of 900°C sintered samples (HLW pH=7, ①②③Fe_2O_3 free, ④⑤⑥9% Fe_2O_3 addition).

For unsintered samples, the addition of Fe_2O_3 lowered the leaching rate slightly while the variation tendency stayed the same with the Fe_2O_3 free samples, which is why the leaching rate of Cs^+ is lower in higher HLW pH value. In an acidic environment, free H^+ makes the MgO dissolve faster and thus sped up the hydration reaction. This makes Fe_2O_3 have fewer chances for entering the crystal lattice or for being absorbed. Thus, harming the immobilization of Cs^+ and making it escape easily from the solidification form. Addition of Fe_2O_3 makes the form more compacted because of the accumulation of its particles. Denser structure prevents the flushing out of the Cs^+.

For sintered samples, sintering at 900°C makes the solidification form a fire ceramic structure. Cs^+ replaces

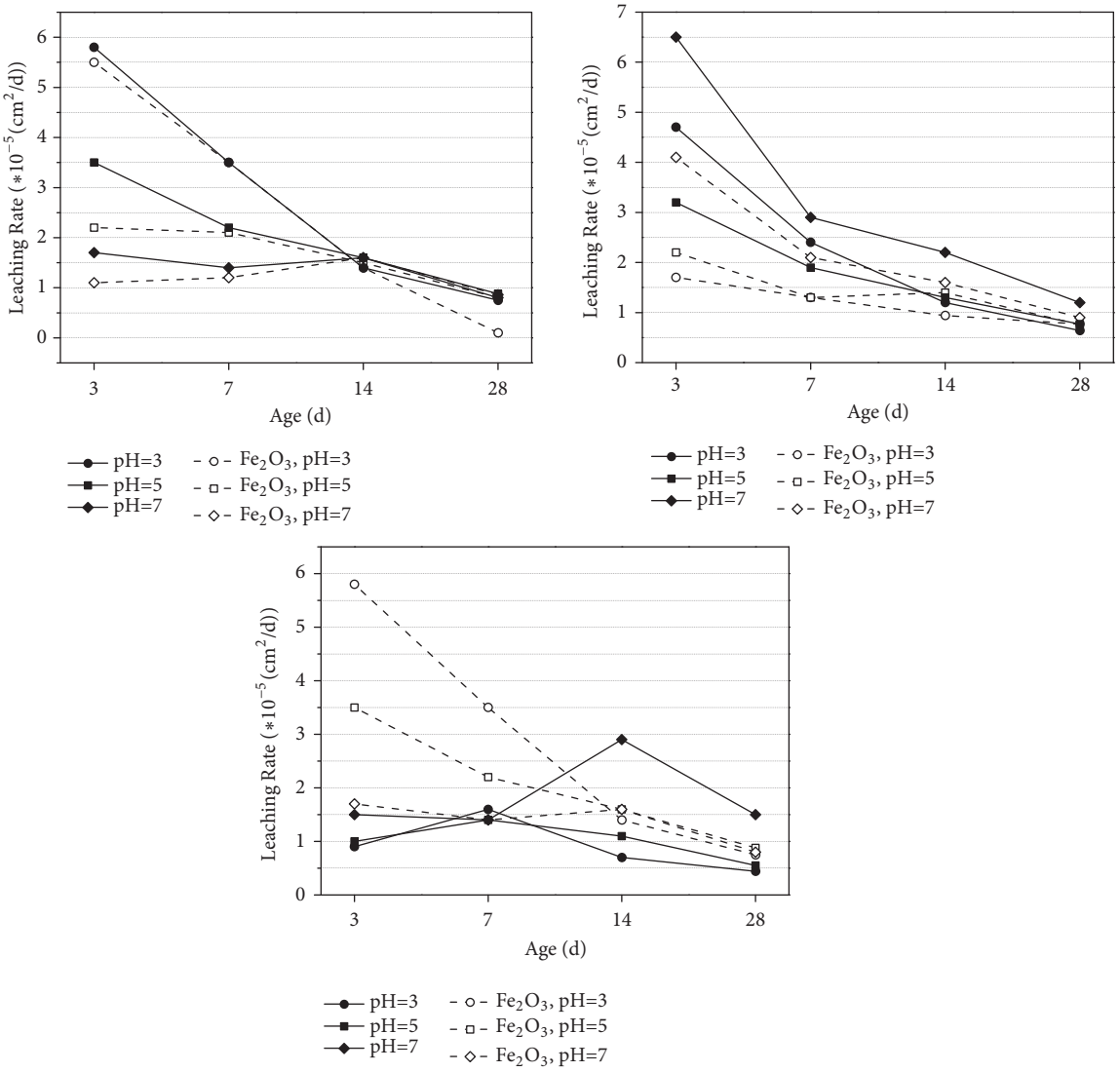

Figure 12: Leaching rate of Cs^+ (①unsintered samples, ② 900°C sintered samples, ③1000°C sintered samples).

K^+ and forms $MgCsPO_4$ and $CsFePO_4$ both of which have better water resistance. The addition of Fe_2O_3 lowered the leaching rate significantly since it lowered the melting point and helped the formation of ceramic.

Sintering at 1000°C cut the Cs^+ leaching rate of Fe_2O_3 free samples but improved the Cs^+ leaching rate of Fe_2O_3 containing samples dramatically. This again proved that the addition of Fe_2O_3 lowered the melting point, destroying Fe_2O_3 containing samples in the 1000°C sintering, and Cs^+ was leached out easily because of the failure of encapsulation and absorption.

4. Conclusions

As an additive for the novel procedure of HLW immobilization, in which the liquid HLW was added to substitute mixing water of the magnesium potassium phosphate cement system, the effect of Fe_2O_3 can be concluded as follows.

Addition of Fe_2O_3 lowers the heat release rate of the hydration reaction significantly, thus lowering the temperature of the mixture during hydration, while not harming the comprehensive strength of the test blocks.

Fe_2O_3 increases the compactness of the samples due to the accumulation of particles. For sintered samples, the existence of Fe_2O_3 lowers the melting point and generates more liquid phase in the sintering; this lowers the firing temperature effectively.

Fe_2O_3 is an inert matter for the hydration reaction, but it plays a positive role in sintering process. It lowers the melting point and helps the formation of ceramic structure. The sintering process produces $CsFe(PO_4)_2$ and immobile Cs^+ more effectively.

When taking its cheap price and remarkable availability into consideration, Fe_2O_3 may play an important role as an additive in the application of HLW immobilization with MKPC.

Data Availability

The raw/processed data required to reproduce these findings cannot be shared at this time due to technical or time limitations.

Conflicts of Interest

The authors declare that all received funding in the "Acknowledgments" section did not lead to any conflicts of interest, and there are no other possible conflicts of interest in the article.

Acknowledgments

The authors would like to acknowledge the financial support listed: International Cooperation Project of National Nature Science Fund of China, Grant No. 0211002321124; Chongqing Municipal Education Commission Science and Technology Planning Project, Grant No. KJ1600636; Student Science and Technology Innovation Fund of Chongqing Technology and Business University, Grant No. 173018; Environmental Pollution Control Team Fund of Environment and Resources College, CTBU.

References

[1] S. E. Vinokurov, Y. M. Kulyako, O. M. Slyuntchev, S. I. Rovny, and B. F. Myasoedov, "Low-temperature immobilization of actinides and other components of high-level waste in magnesium potassium phosphate matrices," *Journal of Nuclear Materials*, vol. 385, no. 1, pp. 189–192, 2009.

[2] I. W. Donald, B. L. Metcalfe, and R. N. J. Taylor, "The immobilization of high level radioactive wastes using ceramics and glasses," *Journal of Materials Science*, vol. 32, no. 22, pp. 5851–5887, 1997.

[3] W. E. Lee, M. I. Ojovan, M. C. Stennett, and N. C. Hyatt, "Immobilisation of radioactive waste in glasses, glass composite materials and ceramics," *Advances in Applied Ceramics*, vol. 105, no. 1, pp. 3–12, 2006.

[4] N. Yamasaki, K. Yanagisawa, S. Kanahara, M. Nishioka, K. Matsuok, and J. Yamazaki, "Immobilization of radioactive wastes in hydrothermal synthetic rock: Lithification of silica powder," *Journal of Nuclear Science and Technology*, vol. 21, no. 1, pp. 71–73, 1984.

[5] N. Yamasaki, K. Yanagisawa, S. Kanahara, M. Nishioka, K. Matsuoka, and J. Yamazaki, "Immobilization of Radioactive Wastes in Hydrothermal Synthetic Rock," in *Hydrothermal Reactions for Materials Science and Engineering: An Overview of Research*, S. Sōmiya, Ed., pp. 348–350, Springer, Dordrecht, Netherlands, 1989.

[6] A. Ringwood, "Immobilization of Radioactive Wastes in SYNROC: A high-performance titanate ceramic waste form composed of minerals that have survived in various natural environments for long periods, SYNROC should permit safe burial of waste in deep drill holes," *American Scientist*, vol. 70, no. 2, pp. 201–207, 1982.

[7] M. Atkins and F. P. Glasser, "Application of portland cement-based materials to radioactive waste immobilization," *Waste Management*, vol. 12, no. 2-3, pp. 105–131, 1992.

[8] N. Liu and B. Chen, "Experimental research on magnesium phosphate cements containing alumina," *Construction and Building Materials*, vol. 121, pp. 354–360, 2016.

[9] B. Kanter, A. Vikman, T. Brückner, M. Schamel, U. Gbureck, and A. Ignatius, "Bone regeneration capacity of magnesium phosphate cements in a large animal model," *Acta Biomaterialia*, vol. 69, pp. 352–361, 2018.

[10] X. Lu and B. Chen, "Experimental study of magnesium phosphate cements modified by metakaolin," *Construction and Building Materials*, vol. 123, pp. 719–726, 2016.

[11] Y. Li, W. Bai, and T. Shi, "A study of the bonding performance of magnesium phosphate cement on mortar and concrete," *Construction and Building Materials*, vol. 142, pp. 459–468, 2017.

[12] Y. Li and B. Chen, "Factors that affect the properties of magnesium phosphate cement," *Construction and Building Materials*, vol. 47, pp. 977–983, 2013.

[13] Y.-S. Wang, J.-G. Dai, L. Wang, D. C. W. Tsang, and C. S. Poon, "Influence of lead on stabilization/solidification by ordinary Portland cement and magnesium phosphate cement," *Chemosphere*, vol. 190, pp. 90–96, 2018.

[14] T. Sugama and L. E. Kukacka, "Magnesium monophosphate cements derived from diammonium phosphate solutions," *Cement and Concrete Research*, vol. 13, no. 3, pp. 407–416, 1983.

[15] D. A. Hall, R. Stevens, and B. El-Jazairi, "The effect of retarders on the microstructure and mechanical properties of magnesia-phosphate cement mortar," *Cement and Concrete Research*, vol. 31, no. 3, pp. 455–465, 2001.

[16] B. Rentsch, A. Bernhardt, A. Henß et al., "Trivalent chromium incorporated in a crystalline calcium phosphate matrix accelerates materials degradation and bone formation in vivo," *Acta Biomaterialia*, vol. 69, pp. 332–341, 2018.

[17] M. Ltifi, A. Guefrech, and P. Mounanga, "Effects of sodium tripolyphosphate addition on early-age physico-chemical properties of cement pastes," *Procedia Engineering*, vol. 10, pp. 1457–1462, 2011.

[18] E. Soudée and J. Péra, "Mechanism of setting reaction in magnesia-phosphate cements," *Cement and Concrete Research*, vol. 30, no. 2, pp. 315–321, 2000.

[19] R. C. Ewing, W. J. Weber, and F. W. Clinard Jr., "Radiation effects in nuclear waste forms for high-level radioactive waste," *Progress in Nuclear Energy*, vol. 29, no. 2, pp. 63–127, 1995.

[20] J. M. Mckibben, "Chemistty of the Purex Process," *Radiochimica Acta*, vol. 36, no. 1-2, 1984.

[21] D. Singh, V. R. Mandalika, S. J. Parulekar, and A. S. Wagh, "Magnesium potassium phosphate ceramic for 99Tc immobilization," *Journal of Nuclear Materials*, vol. 348, no. 3, pp. 272–282, 2006.

[22] A. S. Wagh, R. Strain, S. Y. Jeong, D. Reed, T. Krause, and D. Singh, "Stabilization of Rocky Flats Pu-contaminated ash within chemically bonded phosphate ceramics," *Journal of Nuclear Materials*, vol. 265, no. 3, pp. 295–307, 1999.

[23] A. S. Wagh, S. Y. Sayenko, A. N. Dovbnya et al., "Durability and shielding performance of borated Ceramicrete coatings in beta and gamma radiation fields," *Journal of Nuclear Materials*, vol. 462, pp. 165–172, 2015.

[24] B. C. Sales and L. A. Boatner, "Lead-iron phosphate glass: A stable storage medium for high-level nuclear waste," *Science*, vol. 226, no. 4670, pp. 45–48, 1984.

[25] G. N. Greaves, S. J. Gurman, L. F. Gladden et al., "A structural basis for the corrosion resistance of lead-iron-phosphate glasses: An X-ray absorption spectroscopy study," *Philosophical Magazine*, vol. 58, no. 3, pp. 271–283, 2006.

[26] J. H. Cho, Y. Eom, and T. G. Lee, "Stabilization/solidification of mercury-contaminated waste ash using calcium sodium phosphate (CNP) and magnesium potassium phosphate (MKP) processes," *Journal of Hazardous Materials*, vol. 278, pp. 474–482, 2014.

[27] W. Huang, D. E. Day, C. S. Ray, C.-W. Kim, and A. Mogus-Milankovic, "Vitrification of high chrome oxide nuclear waste in iron phosphate glasses," *Journal of Nuclear Materials*, vol. 327, no. 1, pp. 46–57, 2004.

[28] J. Wang and X. Cao, "Formic denitration of the simulated highlevel liquid waste," *Nuclear Science and Engineering*, no. 01, pp. 93–98, 1997.

[29] D. M. Strachan, R. P. Turcotte, and B. O. Barnes, "MCC-1: A Standard Leach Test for Nuclear Waste Forms," *Nuclear Technology*, vol. 56, no. 2, pp. 306–312, 1980.

[30] W. E. Lee, M. I. Ojovan, and C. M. Jantzen, *Radioactive Waste Management and Contaminated Site Clean-Up*, W. E. Lee, M. I. Ojovan, and C. M. Jantzen, Eds., Woodhead Publishing Limited, 2013.